symmetry

MDPI

Article

Extracting the Parameters of Three-Diode Model of Photovoltaics Using Barnacles Mating Optimizer

Ahmed M. Agwa [1,2,*], Salah K. Elsayed [3] and Ehab E. Elattar [3]

1 Department of Electrical Engineering, Faculty of Engineering, Al-Azhar University, Cairo 11651, Egypt
2 Department of Electrical Engineering, College of Engineering, Northern Border University, Arar 1321, Saudi Arabia
3 Department of Electrical Engineering, College of Engineering, Taif University, P.O. Box 11099, Taif 21944, Saudi Arabia; sabdelhamid@tu.edu.sa (S.K.E.); e.elattar@tu.edu.sa (E.E.E.)
* Correspondence: ah1582009@yahoo.com

Abstract: Modeling of solar generating systems (SGSs) is necessary for recognizing their performance under various conditions of solar irradiance, temperature, and loading. There are nine unbeknown parameters (UPs) in the three-diode model (3-DM); if they are accurately determined, it can exactly identify the real characteristics of SGSs. Parametrization of the 3-DM of SGSs is a nonlinear problem that can be solved via optimization due to its effectivity in determining the optimal parameters to a variety of symmetrical and asymmetrical problems with nonlinearity. Root-mean-squared errors amongst measured and extracted electric current points are the fitness functions to be minimized. The main contributions of this article are the innovative utilization of the barnacles mating optimization algorithm (BMOA) for precise parametrizing of the 3-DM of SGSs and the experimental validation of the SGS. The optimization procedure is based on real measurements of I/V at specific circumstances, in which BMOA is employed to identify the nine UPs of 3-DM of SGSs. Two SGSs are under study, the first of which (Kyocera KC200GT) is widely utilized in the literature for performing comparisons, and the second (Copex P-120) is experimentally set up during different sun irradiances and temperatures. The results of BMOA emphasize its preference over other optimizers for identifying the nine UPs of 3-DM of SGSs.

Keywords: modeling; optimization methods; parameter estimation; photovoltaic cells; solar power generation

Citation: Agwa, A.M.; Elsayed, S.K.; Elattar, E.E. Extracting the Parameters of Three-Diode Model of Photovoltaics Using Barnacles Mating Optimizer. *Symmetry* **2022**, *14*, 1569. https://doi.org/10.3390/sym14081569

Academic Editor: Lorentz JÄNTSCHI

Received: 2 July 2022
Accepted: 25 July 2022
Published: 29 July 2022

1. Introduction

Solar generating systems (SGSs) are promising tools for converting renewable solar energy into electrical energy. SGSs are distinct from other tools since they have shorter setup time, simpler design, longer life, no moving mechanical parts, and no noise [1]. SGSs can be employed either standalone with storage energy or grid-connected. The individual SGS cells generate very low power and voltage (0.5~0.65 V) [2], so groups of standard numbers of SGS cells are connected in series to create a module, which for the same reason is connected in series and parallel groups to create an array [3]. Bifacial SGS can yield energy from both the front side and back side, which can increase the yield energy up to 30% in comparison with traditional monofacial SGS; thus, the energy cost will decrease. Consequently, the SGS industries have recently paid attention to this technology [4].

Three main points (TMP) on the I/V relationship of SGS are commonly declared in datasheets at regular atmospheric condition (RAC) (ambient temperature T_{am} = 20 °C and irradiance G = 1 kW/m^2), namely no-load voltage ($V_{n\text{-}l}$), short-circuit current ($I_{s\text{-}c}$), and voltage ($V_{m\text{-}p}$) with current ($I_{m\text{-}p}$) at maximum power (P_{max}). The aforesaid stated points do not suffice to characterize SGS as proven in the results of this article. The atmospheric conditions vary continuously, so a perfect I/V relationship of SGS at entire statuses is essential to assure an acceptable functioning analysis of SGS during different statuses. The

I/V plots of SGSs can be modeled by one-, two-, and three-diode models (3-DM), which have five, seven, and nine unbeknown parameters (UPs), respectively. The higher the number of diodes in the SGS model, the more precise modeling of the losses [5], so we chose 3-DM for modeling the SGS.

Meanwhile, the application of one of the newest metaheuristic algorithms for parametrizing the 3-DM of SGSs is treated in this article; similar efforts exerted in this regard are surveyed. Many studies have been directed to identify the UPs of the SGS model via numerous optimization algorithms because of its effectiveness in defining the optimum parameters to symmetrical and asymmetrical problems, such as the particle swarm approach [1,6–10], differential evolution (DE) [11–14], farmlands fertility approach [15], support vector machine [16], and counteraction-based sine–cosine approach [17]. Additional modern meta-heuristic-based optimizers, e.g., cuckoo seeking optimizer [18,19], backtracking seeking algorithm [20], imperialist competitive optimizer [21], highest likelihood estimator [22], approximating and correcting procedure [23], Jaya approach [24], interior seeking approach [25], Levenberg–Marquardt optimizer [26], coot optimizer [27], gaining–sharing knowledge algorithm [28], drone squadron algorithm [29], gorilla optimizer [30], and gray wolf optimizer [31] have been utilized to parametrize the SGS model. All of the abovementioned articles treated parametrization of one- and/or two-diode models of SGSs, while some algorithms were employed to parametrize 3-DM of SGSs, namely the sunflower approach (SFA) [5], manta-rays foraging approach (MRFA) [32], Harris hawks algorithm [33], grasshopper optimizer (GO) [34], coyote approach (CA) [35], whale optimizer (WO) [36], marine predator approach [37], and artificial electrical field optimizer [38].

Regarding the above abridged review and complying with the no-free-launch theorem [39], it remains a likelihood to ameliorate the parametrization of the SGS model. For this purpose, this research treats the employment of the barnacles mating optimization algorithm (BMOA) to parametrize the 3-DM of the SGSs. BMOA is one alternative of a metaheuristic; other potential alternatives include the adapted tabu search [40], simulated annealing [41], genetic algorithms [42], and ant colony optimization [43]. BMOA is chosen as it has been innovated recently [44]; in addition, its issued results are encouraging and attest its vantage over other approaches. BMOA is inspired by the mating manner of barnacles in nature to solve optimization topics. Employment of BMOA was successful in optimum reactive power dispatch [44] in addition to economical and emissions dispatch [45].

The contributions of this research are: (i) Innovative employment of BMOA to optimally parametrize the 3-DM of the SGSs; (ii) comparison of BMOA with other approaches via the results of parametrizing 3-DM of the SGS commonly used in the literature; (iii) experimental validation of an actual case study of a commercial SGS module, viz. P-120; (iv) comparison of the 3-DM of the SGS with one- and two-diode models (1- and 2-DMs) via the results of parametrizing them.

The paper is organized as follows: Section 2 displays 3-DM of the SGSs. The fitness function (FF) as well as the constraints are expressed in Section 3. BMOA procedures are stated in Section 4. Materials and methods are presented in Section 5. The yielded results are discussed in Section 6. Validations at changed conditions are presented in Section 7. Conclusions are briefed in Section 8.

2. Modeling the SGS via 3-DM

The nonlinearity of the 3-DM of the SGSs, which is the cause of orientation to optimization for identifying its UPs, is illustrated in this section. The 3-DM of the SGSs, as displayed in Figure 1, is comprised of an electric current source in parallel with three diodes and shunt resistance (R_{sh}). There exist series resistances (R_s) with the mentioned elements. The power losses inside the cell are embodied via R_{sh} and R_s. Applying the current law of Kirchhoff on the equivalent circuit of 3-DM of the SGS leads to:

$$I_{sol} = I_{phot} - I_{D_1} - I_{D_2} - I_{D_3} - \frac{V_{sol} + I_{sol} \cdot R_s}{R_{sh}} \tag{1}$$

$$I_{D_{1\text{-}3}} = I_{rs_{1\text{-}3}}\left[e^{\left(\frac{V_{sol}+I_{sol}\cdot R_s}{M_{1\text{-}3}\cdot V_{th}}\right)} - 1\right] \quad (2)$$

$$V_{th} = \frac{K\cdot T_K}{q} \quad (3)$$

where:

I_{sol} is generated current of SGS cell;
I_{phot} is photo-produced current;
I_D is the current passing in a diode;
V_{sol} is generated voltage of SGS cell;
M is diode quality coefficient, which interprets various mechanisms responsible for moving carriers across the diode junction, M = 1 if the transport process is wholly diffusion, and M ≈ 2 if it is mainly recombination in the depletion zone;
I_{rs} is diode opposite saturated current;
V_{th} is thermic voltage;
K is Boltzmann constant = 1.38065×10^{-23} J/K;
T_K is the cell temperature (K);
q is the electron charge = $1.60217646 \times 10^{-19}$ C.

The module owns N_{ce} series linked cells with gross module voltage (V_{mo}) of $N_{ce}\cdot V_{sol}$ and the module current (I_{mo}) equals I_{sol}, the relationship in module is obtained via modifying (2) as stated in (4).

$$I_{D_{1\text{-}3}} = I_{rs_{1\text{-}3}}\left[e^{\left(\frac{N_{ce}\cdot V_{sol}+I_{sol}\cdot N_{ce}\cdot R_s}{N_{ce}\cdot M_{1\text{-}3}\cdot V_{th}}\right)} - 1\right] \quad (4)$$

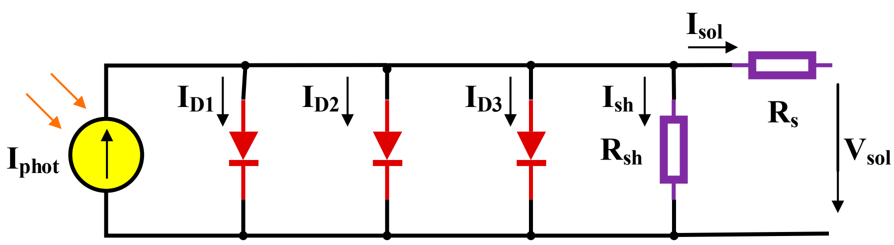

Figure 1. Equivalent circuit of 3-DM of the SGS.

The shunt resistance current for the module (I_{sh}) is calculated using (5).

$$I_{sh} = \frac{V_{mo} + I_{sol}\cdot N_{ce}\cdot R_s}{N_{ce}\cdot R_{sh}} \quad (5)$$

It is recognized that M and R_s do not count on neither G nor T variants [46]. Nevertheless, other variables, viz. I_{phot}, I_{rs}, E_g and R_{sh} count on either G and/or T as detailed below.

I_{phot} principally counts on G and T [47], as stated in (6), knowing that the regular cell temperature throughout testing is 25 °C.

$$I_{phot} = I_{phot\_n}\cdot[1 + K_i\cdot(T - 25)]\cdot\frac{G}{1000} \quad (6)$$

where:

I_{phot_n} is the photo-produced current at RAC;
K_i is the temperature factor of the current;
T is the cell temperature (°C);
I_{rs} counts on T [47–49], as depicted in (7).

$$I_{rs} = I_{rs_n}\left(\frac{T}{25}\right)^3 e^{\left(\frac{q\cdot E_g}{M\cdot K}\right)\left(\frac{1}{25}-\frac{1}{T}\right)} \quad (7)$$

where:

I_{rs_n} is diode reverse-saturation current at RAC;

E_g is band-gap energy;

E_g counts on T that can be modified via (8). The open-circuit voltage is reliant on T as stated in (9).

$$E_g = E_{g_n}\left[1 - 2.668 \times 10^{-4}(T - 25)\right] \quad (8)$$

$$V_{n\text{-}l} = V_{n\text{-}l\_n}[1 + K_v \cdot (T - 25)] \quad (9)$$

where:

E_{g_n} is band-gap energy at RAC;

$V_{n\text{-}l\_n}$ is no-load voltage at RAC;

K_v is the temperature factor of voltage;

Shunt resistance counts on G [46,50] as stated in (10).

$$R_{sh} = R_{sh_n}\left(\frac{1000}{G}\right) \quad (10)$$

where R_{sh_n} is shunt resistance at RAC.

The cell working temperature is nearly defined [51] as depicted in (11).

$$T = T_{am} + \left(\frac{RFCT - 20}{800}\right) \cdot G \quad (11)$$

where RFCT is regular functioning cell temperature (°C).

Regarding (1) to (6), it is obvious that there exist nine Ups, viz. $\left(I_{phot}, I_{rs_{1\text{-}3}}, R_{sh}, R_s, M_{1\text{-}3}\right)$, which need to be identified since they are not prescribed in the datasheets. BMOA is employed to optimize the Ups for owning the fittest values inside their higher and lower limits. Optimization is performed for assurance of precise modeling of SGS aimed at simulation and analysis.

3. Formulating the FF and Its Constraints

The FF to be minimized by BMOA is formulated in this section. FF works toward minimizing the root of the mean-squared errors (RMSEs) amongst the analogous measured and computed electric currents of SGS as depicted in (12).

$$FF = \min(RMSEs) = \min\left\{\sqrt{\frac{1}{N_{me}} \cdot \sum_{m=1}^{N_{me}} \left(I_{M_{me}}(m) - I_{M_{co}}(m)\right)^2}\right\} \quad (12)$$

where:

N_{me} is the number of measurements;

$I_{M_{co}}$ and $I_{M_{me}}$ are the computed and measured current of SGS, respectively.

While scrutinizing (1) and (2), we notice the nonlinearity in (1) as well as the existence of I_{sol} on both sides of (1); this necessitates computing I_{sol} numerically. The Newton–Raphson method is chosen to be utilized via rewriting (1) as zero formula F (I_{sol}) and calculating its derivative $F'(I_{sol})$ with respect to I_{sol}, then I_{sol} can be computed as below:

$$I_{sol_{j+1}} = I_{sol_j} - \frac{F\left(I_{sol_j}\right)}{F'\left(I_{sol_j}\right)} \quad (13)$$

where j is the j^{th} iteration.

The upper and lower limits of $\left(I_{photo}, I_{rs_{1\text{-}3}}, R_{sh}, R_s, M_{1\text{-}3}\right)$ identify the constraints to which the FF is submitted.

4. Overview of the BMOA

Barnacles are aquatic microorganisms which have existed for millions of years. Barnacles ae famous for their penis length (pl) with respect to its body [52], which ranges from seven to eight times its body length to handle being sedentary with the tides. In this research, an innovative optimizer is inspired via the barnacles mating manner, where the elected solution is supposed to be the barnacles and the process is iterated until reaching a predefined number (ite_{max}) as described below:

4.1. Initialization

The solutions are initiated by subjugating to the top and bottom limits, then the population array is written as below:

$$X = \begin{bmatrix} x_1^1 & \cdots & x_1^M \\ \vdots & \ddots & \vdots \\ x_{po}^1 & \cdots & x_{po}^M \end{bmatrix} \tag{14}$$

where:

po is the population number of barnacles;

M is the dimension of the problem to be optimized.

The solutions are sorted in descending arrangement by putting the finest at the top of the array X.

4.2. Selection

BMOA differs from other evolutionary optimizers, e.g., GA, DE, etc. in the selection for mating where a barnacle is selected depending on its pl [45]. The selection in BMOA imitates the barnacles' manner in terms of (i) exploitation—a random selection of females located within the range of pl; (ii) exploration—when the selected female is at distance beyond pl, the sperm is released in the water to fertilize it.

4.3. Reproduction

Reproduction in BMOA has a slight difference from other evolutionary optimizers in that BMOA has no particular formulas for deriving the barnacles' reproduction; offspring production in BMOA chiefly relies on the hereditary characteristics of parents as depicted below:

$$x_i^{M\_new} = p \cdot x_{barnacle\_f}^M + q \cdot x_{barnacle\_m}^M \ \forall\, d \le pl \tag{15}$$

$$x_i^{M\_new} = rand \cdot x_{barnacle\_m}^M \ \forall\, d > pl \tag{16}$$

$$q = p - 1 \tag{17}$$

where:

p and rand are randomized numbers amongst 0 and 1;

p and q are the characteristic proportions of father and mother which are inserted during the generation of the next offspring, consecutively;

$x_{barnacle\_f}^M$, $x_{barnacle\_m}^M$ are solutions of the selected father and mother, consecutively;

d is the distance from father to mother.

Equation (15) pertains exploitation while (16) concerns exploration.

4.4. Influence of pl in BMOA

In BMOA, the decision to change from exploitation and exploration is determined by adjustment of pl [53]. This decision is a significant matter in any optimizer since excess exploitation can cause adhesion in regional optima, whereas excess exploration can result in missing the universal optima [54]. It is found that adjusting the pl to 70% of po gives the best results [44]. All details of the BMOA can be found in [44]. The MATLAB code of BMOA can be found in [55]. Figure 2 exhibits the flowchart of the BMOA for 3-DM of SGS.

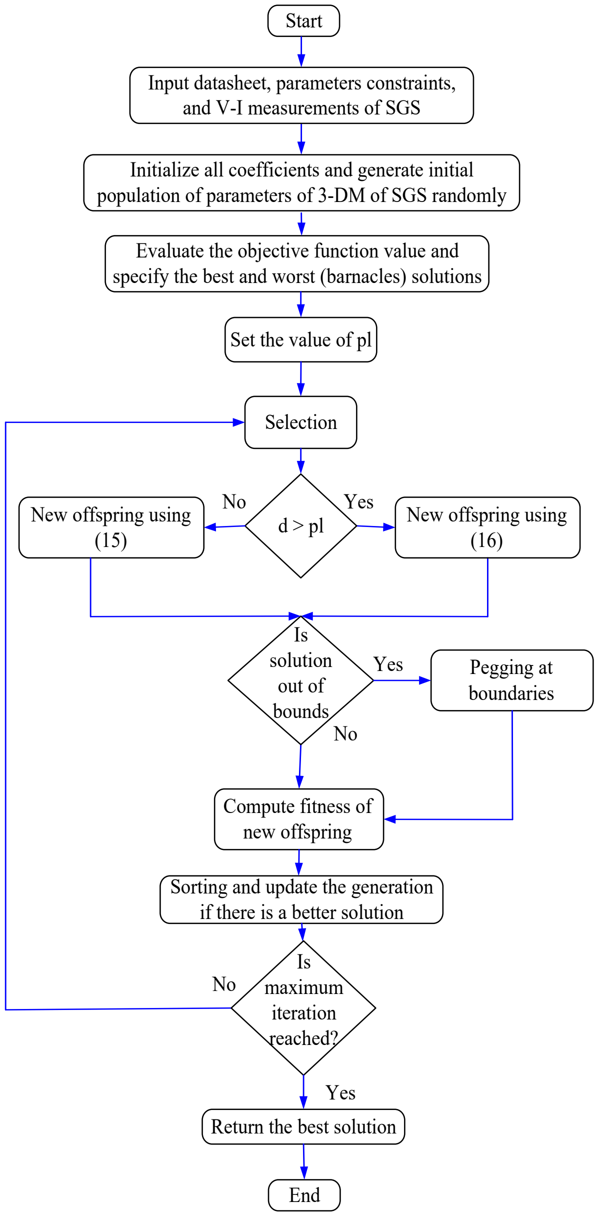

Figure 2. Flowchart of the BMOA for 3-DM of SGS.

5. Materials and Methods

Two modules are under study to assess the efficacy of the proposed BMOA-based procedure in parametrizing the 3-DM of the SGSs. The studied modules are Kyocera KC200GT and Copex P-120. The data of the first module were obtained via ETAP library [56] and the second is experimentally employed and its specifications can be obtained from [57]. The electrical specifications of two SGSs are revealed in Table 1. The limits of the nine UPs of the 3-DM $\left(I_{phot}, I_{rs_{1\text{-}3}}, R_{sh}, R_s, M_{1\text{-}3}\right)$ are listed in Table 2. The simulations are implemented using MATLAB installed on Fujitsu Laptop with an Intel(R) Core ™ i7-4702MQ CPU@ 2.2 GHz 2.2 GHz and RAM of 8 GB.

Table 1. Electrical specifications of SGSs.

Coefficient \ Model	KC200GT [56]	P-120 [57]
P_{max} (W)	200	120
$V_{m\text{-}p}$ (V)	26.3	16.3
$I_{m\text{-}p}$ (A)	7.61	7.37
$V_{n\text{-}l}$ (V)	32.9	19.9
$I_{s\text{-}c}$ (A)	8.21	7.96
N_{ce}	54	32
RFCT (°C)	47	45
K_i (%/°C)	0.000387	0.0006
K_v (%/°C)	−0.003739	−0.0035

Table 2. The bounds of SGS model parameters a cell.

Parameter	Low Bound	High Bound
I_{phot}	0.9 I_{sc}	1.1 I_{sc}
$I_{rs1\text{-}3}$ (μA)	0.001	10
R_{sh} (Ω)	0	500
R_s (Ω)	0	0.5
M_1	1	2
M_2	1.2	2
M_3	1.4	2

Figure 3 exhibits the experimental setup of P-120 SGS, which was held in September 2021 above the building of laboratories in Taif University. Firstly, in this Section, P-120 module is implemented at RAC where G and T are measured via pyranometer and thermometer, respectively. Secondly, P-120 module is implemented at various irradiances and temperatures to exhibit BMOA functioning at various conditions and the results are recorded in Section 6. Potentiometers are employed to load this SGS progressively up to 8 A. Digital multimeters are employed to measure V_{mo} and I_{mo}. Twenty-one points of measurements of V/I are recorded. The equipment class and errors are revealed in Table 3.

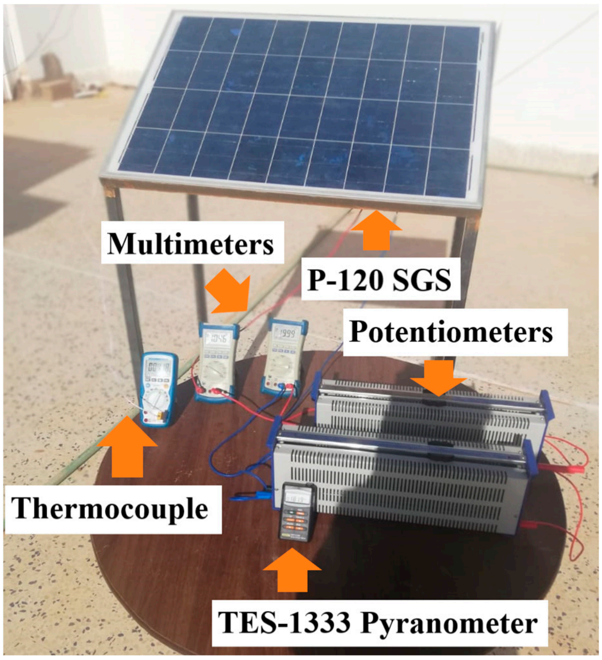

Figure 3. Experimental setup of P-120 SGS module.

Table 3. Equipment class and errors.

Equipment	Class	Error
Pyranometer	TES-1333	5%
Potentiometer	LD-53734	10%
Digital voltmeter	PeakTech-3340	1.2%
Digital Ammeter	PeakTech-3340	2.5%

The ite_{max} is 1000. Table 4 reveals BMOA factors (po, pl) which are defined through trials and errors as followed in all metaheuristic-based optimizers.

Table 4. BMOA factors.

Parameter \ Model	KC200GT	P-120
po	30	30
pl	21	21

6. Results and Discussion

After employing BMOA, the electric currents are computed from the 3-DM; thereafter, RMSEs are calculated via (12), resulting in the smallest value of 9.22045×10^{-2} using all measured points (AMP), which is less than that resulted from other optimizers in the literature by 35.05% to 87.73%, and when TMP is used, the resultant RMSEs are 3.55604×10^{-18}, which are less than that resulted from other optimizers in the literature by 99.91% to 99.99%, as written in Table 5. The benefit of utilizing BMOA for identifying the nine UPs of the 3-DM of SGSs is obvious since the minimum decrease in RMSEs is 35.05% using AMP and 99.91% using TMP. The fittest values of the UPs of the 3-DM are acquired after numerous independent runs of BMOA producing minimum FF because of the stochastic nature of these optimizers. The convergence tendency of the RMSEs diagram is displayed in Figure 4.

Table 5. RMSEs of 3-DM of KC200GT compared to other algorithms.

Approach	AMP			TMP		
	ite_{max}	RMSEs (A)	BMOA Is Less by	ite_{max}	RMSEs (A)	BMOA Is Less by
SFA [5]	1000	3.1746×10^{-2}	54.61%	1000	1.23×10^{-12}	99.91%
MRFA [32]	10,000	2.2185×10^{-2}	35.05%	10,000	7.0673×10^{-5}	99.99%
GO [34]	1000	Not reported	Not reported	1000	9.9775×10^{-11}	99.99%
CA [35]	1000	8.6149×10^{-2}	83.27%	1000	3.357×10^{-11}	99.99%
WO [36]	500	11.74×10^{-2}	87.73%	500	9.8488×10^{-8}	99.99%
BMOA	1000	1.441×10^{-2}	–	1000	1.1471×10^{-15}	–

There are no results in the literature about the P-120 module that was experienced for our article. For validating the BMOA results, two additional optimizers are used, viz. the equilibrium optimizer (EO) [58] and differential search optimizer (DSO) [59] with po = 30 and $ite_{max} = 1000$ as adjusted for BMOA to associate the comparison with fairness.

Comparisons between BMOA, EO, and DSO dependent on the results show that the obtained RMSEs by BMOA own the lowest value, namely 9.22045×10^{-2} using AMP, which is less than that which resulted from other optimizers in the literature by 11.18% to 20.73%, and when TMP is used, the resultant RMSEs are 3.55604×10^{-18}, which is less than that which resulted from other optimizers in the literature by 99.99%. The advantage of utilizing BMOA for identifying the nine UPs of the 3-DM of SGSs is clear, since the minimum decrease in RMSEs is 11.18% using AMP and 99.99% using TMP, as revealed in Figure 5 and Table 6.

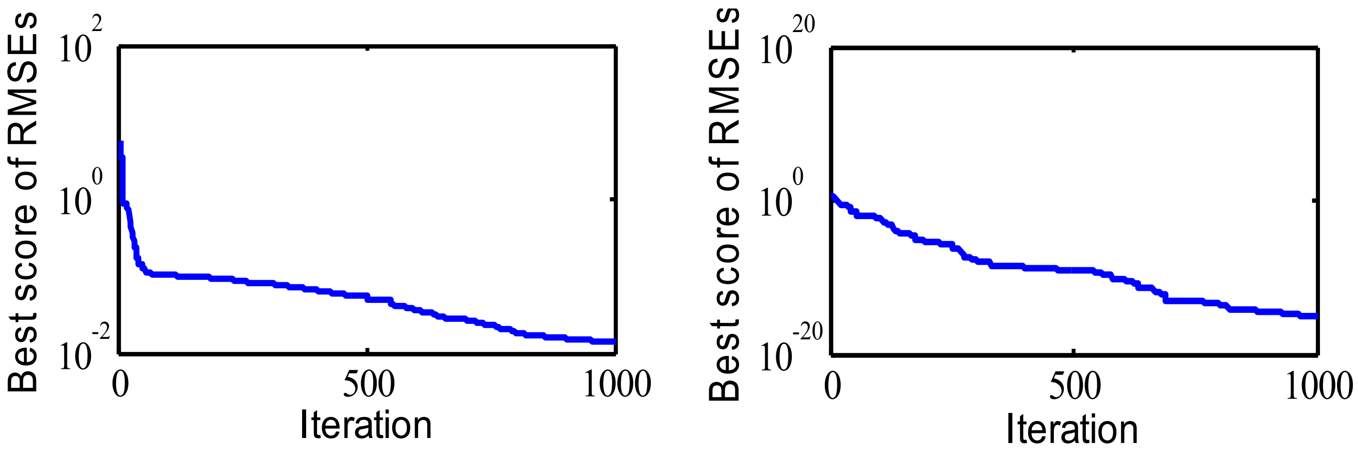

(**a**) AMP (**b**) TMP

Figure 4. RMSEs' convergence for KC200GT.

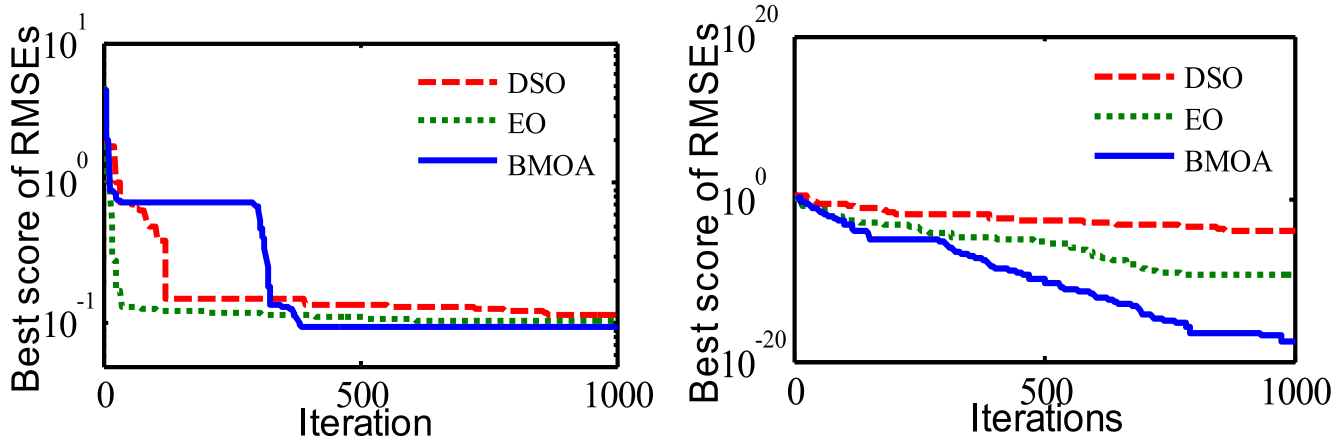

(**a**) AMP (**b**) TMP

Figure 5. RMSEs' convergence for P-120.

Table 6. RMSEs of 3-DM of P-120 compared to other algorithms.

Approach	**AMP**			**TMP**		
	ite_{max}	**RMSEs (A)**	**BMOA Is Less by**	**ite_{max}**	**RMSEs (A)**	**BMOA Is Less by**
EO [51]	1000	10.381×10^{-2}	11.18%	1000	4.87048×10^{-10}	99.99%
DSO [52]	1000	11.6317×10^{-2}	20.73%	1000	8.2725×10^{-5}	99.99%
BMOA	1000	9.22045×10^{-2}	–	1000	3.55604×10^{-18}	–

Extracted UPs per cell of the 3-DM of the SGSs using AMP are written in Table 7. With reference to (5) and (6), it is clear that the total module parameters, namely shunt, series resistors, and diode quality coefficient, can be computed as R_{sh}/module = N_{ce} × (R_{sh}/cell), R_s/module = N_{ce} × (R_s/cell), and $M_{1\text{-}3}$/module = N_{ce} × ($M_{1\text{-}3}$/cell), respectively. The RMSEs convergences are revealed in Figures 4 and 5. The convergence variability among the different SGSs is due to different ratings of power, voltage, and current and accordingly different measurements. Additionally, the stochastic nature of the optimizer leads to convergence variability among the different SGSs.

Table 7. Extracted UPs of the 3-DM of the SGSs.

Parameter \ Model	KC200GT	P-120
I_{phot} (A)	8.1996	8.5067
I_{rs_1} (μA)	0.001	0.0014
I_{rs_2} (μA)	0.0016	0.0483
I_{rs_3} (μA)	0.0037	0.0903
R_{sh} (Ω)	143.0839	500
R_s (Ω)	0.24539	0.0105
M_1	1.0475	1
M_2	1.9668	1.2
M_3	2	2

The yielded results for the I/V plot of SGS at RAC that are extracted by BMOA using AMP and the measured values are displayed in Figures 6a and 7a, for KC200GT and P-120 modules, correspondingly. Closeness amongst the experienced electric currents and calculated electric currents by BMOA affirms the precision of the estimated UPs of the 3-DM of the SGSs. While similar results are extracted by BMOA using TMP (Figures 6b and 7b), there is less closeness despite the RMSEs being smaller, since RMSEs are computed only at TMP, which prove that TMP does not suffice to characterize SGS, as mentioned in Section 1.

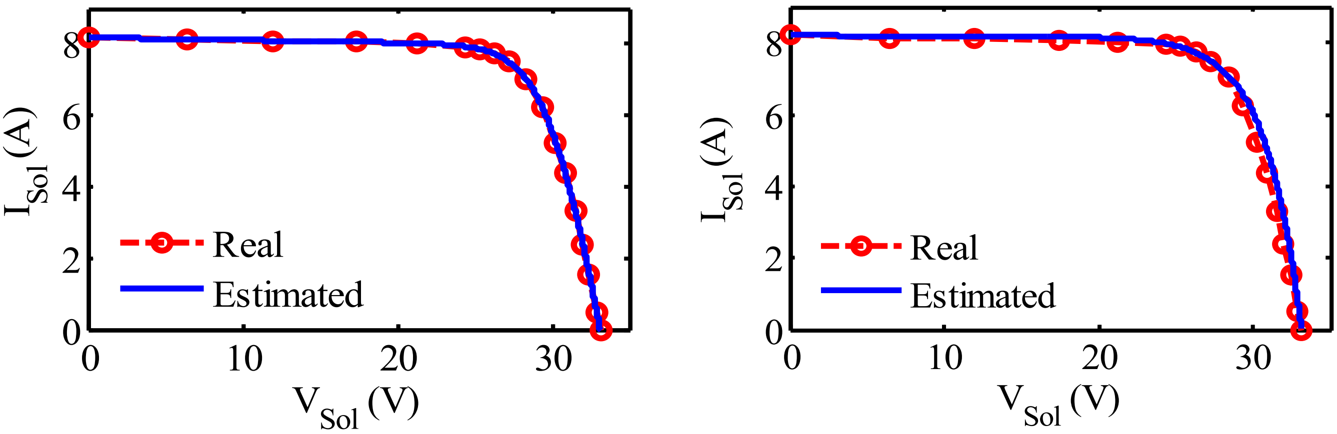

(**a**) AMP (**b**) TMP

Figure 6. I/V plots of KC200Gtwith AMP and TMP using BMOA against actual measurements.

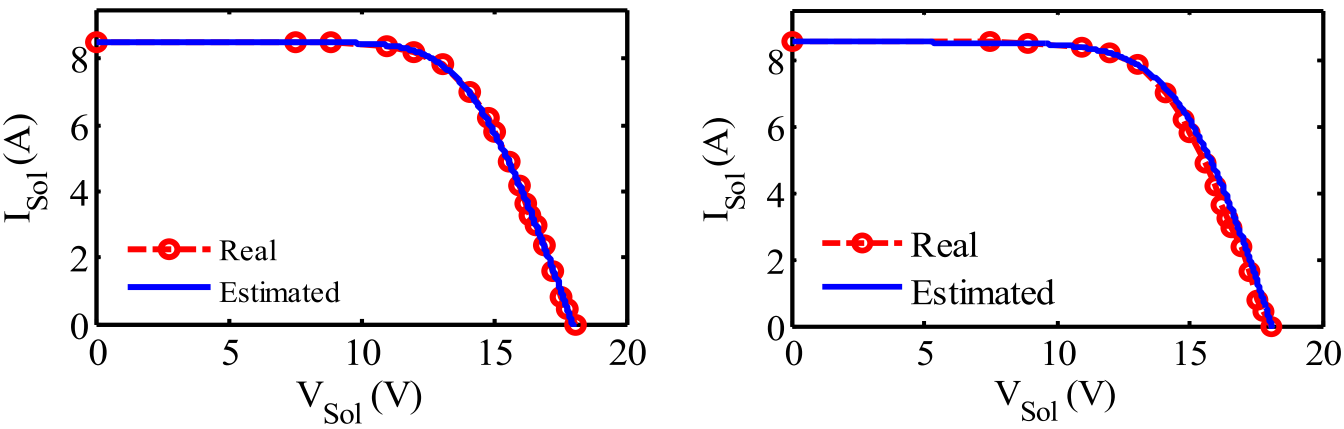

(**a**) AMP (**b**) TMP

Figure 7. I/V plots of P-120 with AMP and TMP using BMOA against actual measurements.

In the same manner, the P/V plots are displayed in Figures 8a and 9a for KC200GT and P-120 modules using AMP, correspondingly, while Figures 8b and 9b display the P/V plots using TMP. Once more, well-coinciding amongst 3-DM along with the analogous measured values is recognized when using AMP more than that when using TMP. Operational measures are prepared through parametric tests to attest the dynamism of the BMOA results using AMP.

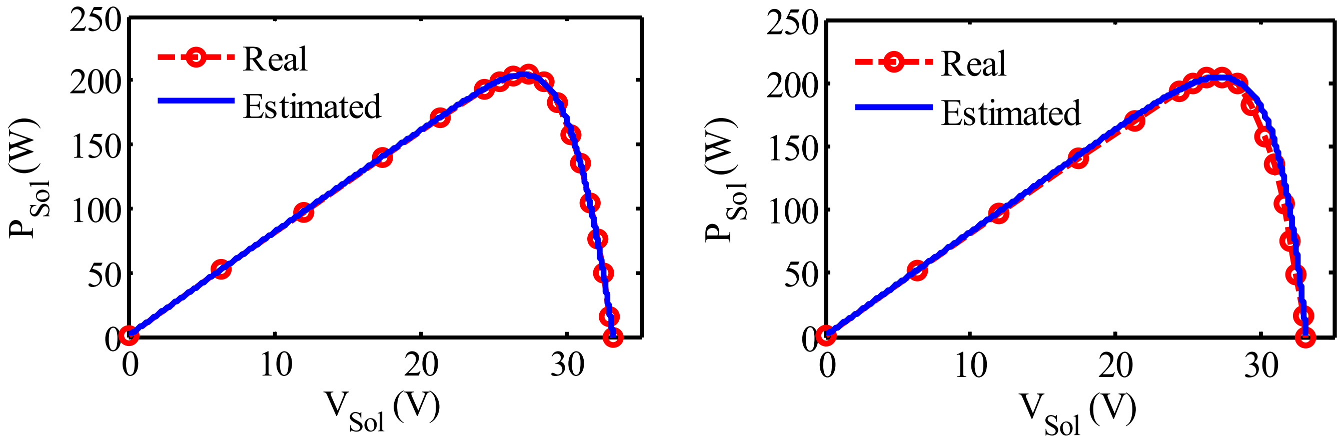

(**a**) AMP (**b**) TMP

Figure 8. P/V plots of KC200GT with AMP and TMP using BMOA against actual measurements.

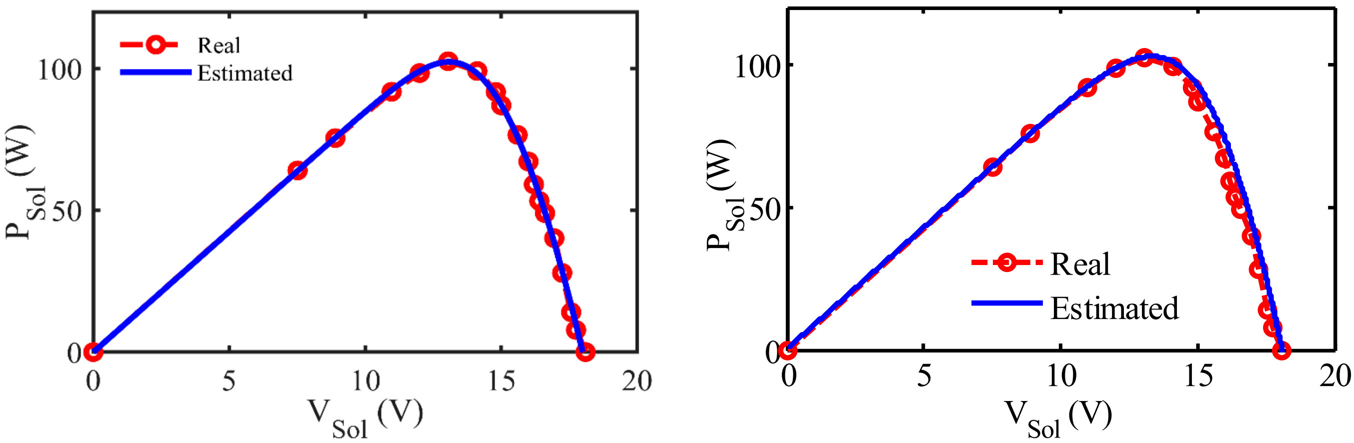

(**a**) AMP (**b**) TMP

Figure 9. P/V plots of P-120with AMP and TMP using BMOA against actual measurements.

Table 8 abridges the BMOA procedures along 100 autonomous runs and associated pointers, namely best, mean, worst, and standard deviation (SD) of RMSE values. It can be said that the lesser SDs affirm the dynamism of the cropped results and manifest the delicate choice of adjusted BMOA factors.

Table 8. RMSEs statistical results.

Factor	KC200GT	P-120
RMSE (Best)	1.441×10^{-2}	9.22045×10^{-2}
RMSE (Mean)	1.4783×10^{-2}	9.54783×10^{-2}
RMSE (Worst)	1.5368×10^{-2}	9.9369×10^{-2}
RMSE (SD)	2.8886×10^{-4}	5.61615×10^{-4}

After comparing BMOA with other optimizers to identify the nine UPs of the 3-DM of SGSs, the 3-DM of SGSs needs to be proven to have the most precise modeling of the losses by comparing it with the 1- and 2-DMs of KC200GT, as written in Table 9. Comparisons between the 1-, 2-, and 3-DMs of SGSs dependent on the results show that the obtained RMSEs using BMOA via the 3-DM have the lowest value, namely 1.441×10^{-2} which is less than that which resulted from the 1- and 2-DMs by 85.93% and 88.46%, respectively.

Table 9. RMSEs using BMOA via 3-DM of KC200GT compared to 1- and 2-DMs.

Model	RMSEs (A)	3-DM Is Less by
1-DM [60]	10.244×10^{-2}	85.93%
2-DM [60]	12.492×10^{-2}	88.46%
3-DM	1.441×10^{-2}	–

7. Validations at Different Solar Irradiances and Temperatures

The I/V and P/V plots of the P-120 SGS module need to be measured at various irradiances and temperatures to show that the extracted Ups of the 3-DM of SGSs using BMOA at RAC are functioning efficiently at various conditions. In Figure 10, G is 1000 W/m^2, 800 W/m^2, and 600 W/m^2, while T has a constant value of 25 °C. It is seen that the irradiance augmentation leads to an increase in the produced current and power of SGS.

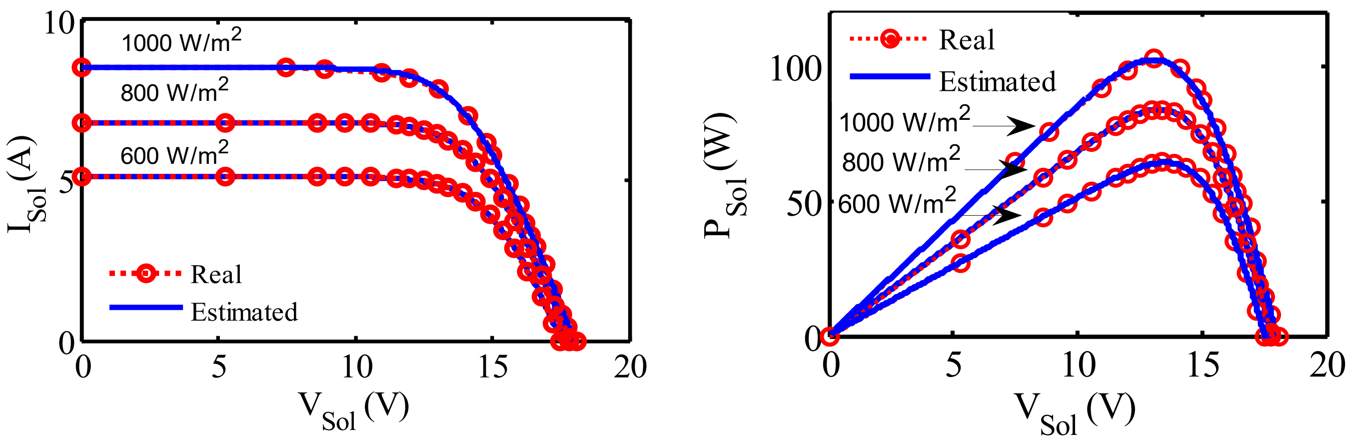

(**a**) I/V plot (**b**) P/V plot

Figure 10. Procedure characteristic of P-120 with 3-DM using BMOA at various irradiances.

Subsequently, the influence of temperature variation is displayed in Figure 11, where T is 40 °C and 25 °C, (while G has a constant value of 1000 W/m^2). It is apparent that the rise in temperature causes a reduction in the produced voltage and power of the SGS module.

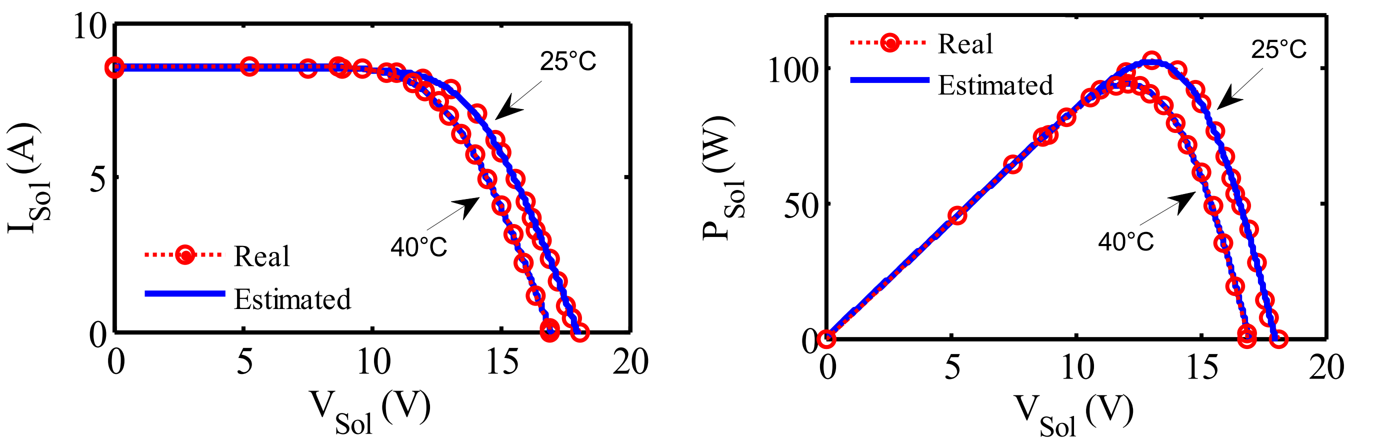

(**a**) I/V plot (**b**) P/V plot

Figure 11. Procedure characteristic of P-120 with 3-DM using BMOA at various temperatures.

8. Conclusions

In this research, the innovative employment of a newly designed BMOA approach was executed to extract the UPs of the 3-DM of SGSs. The purpose is the development of an efficacious model of the SGSs that provides accurate simulation and modeling during various conditions. The FF is to minimize the root of the mean-squared errors amongst the analogous measured and computed electric-current values of SGS succumbed to constraints, which are identified though the low and high bounds of parameters. Appraisal of the suggested model's effectiveness has been carried out by comparing its estimated results with the experimental results of two commercial SGSs. The first SGS is obtained from the literature for comparisons, while the second SGS is experimentally set up. The estimated results are consistent with the experimental results in whole case studies. Moreover, comparisons amongst the BMOA-obtained results and other optimizers' results have been conducted. The RMSEs that resulted from BMOA are lower than those which resulted from other optimizers by 11.18% to 87.73% using AMP and by 99.91% to 99.99% using TMP. Thus, the results display a high rivalry of the BMOA to other approaches in the literature and evidence its applicability. Finally, the 3-DM of SGSs has been proven to have the most precise modeling of the losses by comparing it with the 1- and 2-DMs, where the obtained RMSEs using BMOA via 3-DM are lower than those which resulted from the 1- and 2-DMs by 85.93% and 88.46%, respectively.

Author Contributions: Conceptualization, A.M.A.; Data curation, S.K.E. and E.E.E.; Validation, S.K.E. and E.E.E.; Formal analysis, A.M.A.; Funding acquisition, E.E.E.; Investigation, A.M.A.; Methodology, A.M.A.; Project administration, A.M.A.; Resources, S.K.E. and E.E.E.; Software, A.M.A.; Visualization, S.K.E.; Writing—original draft, A.M.A. and S.K.E.; Writing—review & editing, E.E.E. All authors have read and agreed to the published version of the manuscript.

Funding: This work was supported by Taif University Researchers Supporting Project number (TURSP-2020/86), Taif University, Taif, Saudi Arabia.

Data Availability Statement: Not applicable.

Acknowledgments: The authors would like to acknowledge the financial support received from Taif University Researchers Supporting Project Number (TURSP-2020/86), Taif University, Taif, Saudi Arabia.

Conflicts of Interest: The authors declare no conflict of interest.

References

1. Yousri, D.; Allam, D.; Eteiba, M.; Suganthan, P.N. Static and dynamic photovoltaic models' parameters identification using Chaotic Heterogeneous Comprehensive Learning Particle Swarm Optimizer variants. *Energy Convers. Manag.* **2019**, *182*, 546–563. [CrossRef]
2. Al Tarabsheh, A.; Akmal, M.; Ghazal, M. Series Connected Photovoltaic Cells—Modelling and Analysis. *Sustainability* **2017**, *9*, 371. [CrossRef]
3. Yang, W.; Prabhakar, R.R.; Tan, J.; Tilley, S.D.; Moon, J. Strategies for enhancing the photocurrent, photovoltage, and stability of photoelectrodes for photoelectrochemical water splitting. *Chem. Soc. Rev.* **2019**, *48*, 4979–5015. [CrossRef] [PubMed]
4. Sun, X.; Khan, M.R.; Hanna, A.; Hussain, M.M.; Alam, M.A. The Potential of Bifacial Photovoltaics: A Global Perspective. In Proceedings of the 2017 IEEE 44th Photovoltaic Specialist Conference (PVSC), Washington, DC, USA, 25–30 June 2017; pp. 1055–1057. [CrossRef]
5. Qais, M.H.; Hasanien, H.M.; Alghuwainem, S. Identification of electrical parameters for three-diode photovoltaic model using analytical and sunflower optimization algorithm. *Appl. Energy* **2019**, *250*, 109–117. [CrossRef]
6. Nunes, H.; Pombo, J.; Bento, P.; Mariano, S.; Calado, M. Collaborative swarm intelligence to estimate PV parameters. *Energy Convers. Manag.* **2019**, *185*, 866–890. [CrossRef]
7. Nunes, H.; Pombo, J.; Mariano, S.; Calado, M.; de Souza, J.F. A new high performance method for determining the parameters of PV cells and modules based on guaranteed convergence particle swarm optimization. *Appl. Energy* **2018**, *211*, 774–791. [CrossRef]
8. Jordehi, A.R. Time varying acceleration coefficients particle swarm optimisation (TVACPSO): A new optimisation algorithm for estimating parameters of PV cells and modules. *Energy Convers. Manag.* **2016**, *129*, 262–274. [CrossRef]
9. Ma, J.; Man, K.L.; Guan, S.-U.; Ting, T.O.; Wong, P.W.H. Parameter estimation of photovoltaic model via parallel particle swarm optimization algorithm. *Int. J. Energy Res.* **2016**, *40*, 343–352. [CrossRef]
10. Liang, J.; Ge, S.; Qu, B.; Yu, K.; Liu, F.; Yang, H.; Wei, P.; Li, Z. Classified perturbation mutation based particle swarm optimization algorithm for parameters extraction of photovoltaic models. *Energy Convers. Manag.* **2020**, *203*, 112138. [CrossRef]
11. Jiang, L.L.; Maskell, D.L.; Patra, J.C. Parameter estimation of solar cells and modules using an improved adaptive differential evolution algorithm. *Appl. Energy* **2013**, *112*, 185–193. [CrossRef]
12. Chin, V.J.; Salam, Z. A New Three-point-based Approach for the Parameter Extraction of Photovoltaic Cells. *Appl. Energy* **2019**, *237*, 519–533. [CrossRef]
13. Yang, X.; Gong, W.; Wang, L. Comparative study on parameter extraction of photovoltaic models via differential evolution. *Energy Convers. Manag.* **2019**, *201*, 112113. [CrossRef]
14. Li, S.; Gu, Q.; Gong, W.; Ning, B. An enhanced adaptive differential evolution algorithm for parameter extraction of photovoltaic models. *Energy Convers. Manag.* **2020**, *205*, 112443. [CrossRef]
15. Agwa, A.M.; El-Fergany, A.A.; Maksoud, H.A. Electrical characterization of photovoltaic modules using farmland fertility optimizer. *Energy Convers. Manag.* **2020**, *217*, 112990. [CrossRef]
16. Harrou, F.; Dairi, A.; Taghezouit, B.; Sun, Y. An unsupervised monitoring procedure for detecting anomalies in photovoltaic systems using a one-class Support Vector Machine. *Sol. Energy* **2019**, *179*, 48–58. [CrossRef]
17. Chen, H.; Jiao, S.; Heidari, A.A.; Wang, M.; Chen, X.; Zhao, X. An opposition-based sine cosine approach with local search for parameter estimation of photovoltaic models. *Energy Convers. Manag.* **2019**, *195*, 927–942. [CrossRef]
18. Chen, X.; Yu, K. Hybridizing cuckoo search algorithm with biogeography-based optimization for estimating photovoltaic model parameters. *Sol. Energy* **2019**, *180*, 192–206. [CrossRef]
19. Kang, T.; Yao, J.; Jin, M.; Yang, S.; Duong, T. A Novel Improved Cuckoo Search Algorithm for Parameter Estimation of Photovoltaic (PV) Models. *Energies* **2018**, *11*, 1060. [CrossRef]
20. Zhang, Y.; Jin, Z.; Zhao, X.; Yang, Q. Backtracking search algorithm with Lévy flight for estimating parameters of photovoltaic models. *Energy Convers. Manag.* **2020**, *208*, 112615. [CrossRef]
21. Fathy, A.; Rezk, H. Parameter estimation of photovoltaic system using imperialist competitive algorithm. *Renew. Energy* **2017**, *111*, 307–320. [CrossRef]
22. Ayang, A.; Wamkeue, R.; Ouhrouche, M.; Djongyang, N.; Salomé, N.E.; Pombe, J.K.; Ekemb, G. Maximum likelihood parameters estimation of single-diode model of photovoltaic generator. *Renew. Energy* **2019**, *130*, 111–121. [CrossRef]
23. Muhammad, F.F.; Sangawi, A.W.K.; Hashim, S.; Ghoshal, S.K.; Abdullah, I.K.; Hameed, S.S. Simple and efficient estimation of photovoltaic cells and modules parameters using approximation and correction technique. *PLoS ONE* **2019**, *14*, e0216201. [CrossRef] [PubMed]
24. Yu, K.; Qu, B.; Yue, C.; Ge, S.; Chen, X.; Liang, J. A performance-guided JAYA algorithm for parameters identification of photovoltaic cell and module. *Appl. Energy* **2019**, *237*, 241–257. [CrossRef]
25. Kler, D.; Goswami, Y.; Rana, K.; Kumar, V. A novel approach to parameter estimation of photovoltaic systems using hybridized optimizer. *Energy Convers. Manag.* **2019**, *187*, 486–511. [CrossRef]
26. Blaifi, S.-A.; Moulahoum, S.; Taghezouit, B.; Saim, A. An enhanced dynamic modeling of PV module using Levenberg-Marquardt algorithm. *Renew. Energy* **2019**, *135*, 745–760. [CrossRef]
27. Gouda, E.A.; Kotb, M.F.; Ghoneim, S.S.M.; Al-Harthi, M.M.; El-Fergany, A.A. Performance Assessment of Solar Generating Units Based on Coot Bird Metaheuristic Optimizer. *IEEE Access* **2021**, *9*, 111616–111632. [CrossRef]

28. Sallam, K.M.; Hossain, A.; Chakrabortty, R.K.; Ryan, M.J. An improved gaining-sharing knowledge algorithm for parameter extraction of photovoltaic models. *Energy Convers. Manag.* **2021**, *237*, 114030. [CrossRef]
29. Gnetchejo, P.J.; Essiane, S.N.; Dadjé, A.; Ele, P. A combination of Newton-Raphson method and heuristics algorithms for parameter estimation in photovoltaic modules. *Heliyon* **2021**, *7*, e06673. [CrossRef]
30. Ginidi, A.; Ghoneim, S.M.; Elsayed, A.; El-Sehiemy, R.; Shaheen, A.; El-Fergany, A. Gorilla Troops Optimizer for Electrically Based Single and Double-Diode Models of Solar Photovoltaic Systems. *Sustainability* **2021**, *13*, 9459. [CrossRef]
31. Xavier, F.J.; Pradeep, A.; Premkumar, M.; Kumar, C. Orthogonal learning-based Gray Wolf Optimizer for identifying the uncertain parameters of various photovoltaic models. *Optik* **2021**, *247*, 167973. [CrossRef]
32. El-Hameed, M.A.; Elkholy, M.M.; El-Fergany, A.A. Three-diode model for characterization of industrial solar generating units using Manta-rays foraging optimizer: Analysis and validations. *Energy Convers. Manag.* **2020**, *219*, 113048. [CrossRef]
33. Qais, M.H.; Hasanien, H.M.; Alghuwainem, S. Parameters extraction of three-diode photovoltaic model using computation and Harris Hawks optimization. *Energy* **2020**, *195*, 117040. [CrossRef]
34. Elazab, O.S.; Hasanien, H.M.; Alsaidan, I.; Abdelaziz, A.Y.; Muyeen, S.M. Parameter Estimation of Three Diode Photovoltaic Model Using Grasshopper Optimization Algorithm. *Energies* **2020**, *13*, 497. [CrossRef]
35. Qais, M.; Hasanien, H.M.; Alghuwainem, S.; Nouh, A.S. Coyote optimization algorithm for parameters extraction of three-diode photovoltaic models of photovoltaic modules. *Energy* **2019**, *178*, 116001. [CrossRef]
36. Elazab, O.S.; Hasanien, H.M.; Elgendy, M.A.; Abdeen, A.M. Parameters estimation of single- and multiple-diode photovoltaic model using whale optimisation algorithm. *IET Renew. Power Gener.* **2018**, *12*, 1755–1761. [CrossRef]
37. Soliman, M.A.; Hasanien, H.M.; Alkuhayli, A. Marine Predators Algorithm for Parameters Identification of Triple-Diode Photovoltaic Models. *IEEE Access* **2020**, *8*, 155832–155842. [CrossRef]
38. Selem, S.I.; El-Fergany, A.A.; Hasanien, H.M. Artificial electric field algorithm to extract nine parameters of triple-diode photovoltaic model. *Int. J. Energy Res.* **2020**, *45*, 590–604. [CrossRef]
39. Wolpert, D.H.; Macready, W.G. No free lunch theorems for optimization. *IEEE Trans. Evol. Comput.* **1997**, *1*, 67–82. [CrossRef]
40. Fava, L.P.; Furtado, J.C.; Helfer, G.A.; Barbosa, J.L.V.; Beko, M.; Correia, S.D.; Leithardt, V.R.Q. A Multi-Start Algorithm for Solving the Capacitated Vehicle Routing Problem with Two-Dimensional Loading Constraints. *Symmetry* **2021**, *13*, 1697. [CrossRef]
41. Yenchamchalit, K.; Kongjeen, Y.; Prabpal, P.; Bhumkittipich, K. Optimal Placement of Distributed Photovoltaic Systems and Electric Vehicle Charging Stations Using Metaheuristic Optimization Techniques. *Symmetry* **2021**, *13*, 2378. [CrossRef]
42. Bolboacă, S.D.; Roşca, D.; Jäntschi, L. Structure-Activity Relationships from Natural Evolution. *Match* **2014**, *71*, 149–172.
43. Lin, Z.; Cao, Y.; Liu, H.; Li, J.; Zhao, S. Research on Optimization of Urban Public Transport Network Based on Complex Network Theory. *Symmetry* **2021**, *13*, 2436. [CrossRef]
44. Sulaiman, M.H.; Mustaffa, Z.; Saari, M.M.; Daniyal, H. Barnacles Mating Optimizer: A new bio-inspired algorithm for solving engineering optimization problems. *Eng. Appl. Artif. Intell.* **2020**, *87*, 103330. [CrossRef]
45. Sulaiman, M.H.; Mustaffa, Z.; Aliman, O. An Application of Barnacles Mating Optimizer for Solving Economic Dispatch Problems. In Proceedings of the 2019 IEEE Jordan International Joint Conference on Electrical Engineering and Information Technology (JEEIT), Amman, Jordan, 9–11 April 2019; pp. 835–839. [CrossRef]
46. Ghani, F.; Rosengarten, G.; Duke, M.; Carson, J. The numerical calculation of single-diode solar-cell modelling parameters. *Renew. Energy* **2014**, *72*, 105–112. [CrossRef]
47. Laudani, A.; Fulginei, F.R.; Salvini, A. High performing extraction procedure for the one-diode model of a photovoltaic panel from experimental I–V curves by using reduced forms. *Sol. Energy* **2014**, *103*, 316–326. [CrossRef]
48. Yahya-Khotbehsara, A.; Shahhoseini, A. A fast modeling of the double-diode model for PV modules using combined analytical and numerical approach. *Sol. Energy* **2018**, *162*, 403–409. [CrossRef]
49. Al-Rashidi, M.R.; El-Naggar, K.M.; Al-Hajri, M.F. Heuristic Approach for Estimating the Solar Cell Parameters. In Proceedings of the 5th WSEAS World Congress on Applied Computing Conference (ACC '12), Faro, Portugal, 2–4 May 2012; pp. 80–83.
50. Carrero, C.; Ramírez, D.; Rodríguez, J.; Platero, C. Accurate and fast convergence method for parameter estimation of PV generators based on three main points of the I–V curve. *Renew. Energy* **2011**, *36*, 2972–2977. [CrossRef]
51. Masters, G.M. *Renewable and Efficient Electric Power Systems*, 2nd ed.; John Wiley & Sons, Inc.: Hoboken, NJ, USA, 2013.
52. Barazandeh, M.; Davis, C.; Neufeld, C.; Coltman, D.; Palmer, A.R. Something Darwin didn't know about barnacles: Spermcast mating in a common stalked species. *Proc. R. Soc. B Boil. Sci.* **2013**, *280*, 20122919. [CrossRef] [PubMed]
53. Sulaiman, M.H.; Mustaffa, Z.; Saari, M.M.; Mohamad, A.J. Barnacles Mating Optimizer for Loss Minimization of Optimal Reactive Power Dispatch. *Prz. Elektrotechniczny* **2022**, *98*, 59–63. [CrossRef]
54. Sulaiman, M.H.; Mustaffa, Z.; Saar, M.M. Using the Barnacles Mating Optimizer for Economic Emission Load Dispatch Problems. *Prz. Elektrotechniczny* **2020**, *96*, 141–144. [CrossRef]
55. Available online: https://drive.google.com/file/d/1OfV_lIWee97Gc2xVz1BGqSS7jHeQHCLd/view (accessed on 7 August 2021).
56. ETAP Powering Success, "ETAP Ver. 18.00". Available online: http://www.ETAP.com/ (accessed on 4 September 2021).
57. Copex P-120, Module. Available online: https://www.enfsolar.com/pv/panel-datasheet/crystalline/32879 (accessed on 10 September 2021).
58. Faramarzi, A.; Heidarinejad, M.; Stephens, B.; Mirjalili, S. Equilibrium optimizer: A novel optimization algorithm. *Knowl.-Based Syst.* **2019**, *191*, 105190. [CrossRef]

59. Civicioglu, P. Transforming geocentric cartesian coordinates to geodetic coordinates by using differential search algorithm. *Comput. Geosci.* **2012**, *46*, 229–247. [CrossRef]
60. Rizk-Allah, R.M.; El-Fergany, A.A. Conscious neighborhood scheme-based Laplacian barnacles mating algorithm for parameters optimization of photovoltaic single- and double-diode models. *Energy Convers. Manag.* **2020**, *226*, 113522. [CrossRef]